

**STRUCTURAL, OPTICAL ABSORBANCE AND TRANSMITTANCE
PROPERTIES OF SILAR DEPOSITED IRON LEAD SULPHIDE(PbSFe) AND
IRONCOPPER SULPHIDE(CuSFe) THIN FILMS**

Udejah, V.N. and Onah, D.U

Department of Industrial Physics

Ebonyi State University, Abakaliki

Email: vakadujah45 @ gmail.com, d_onah @yahoo.co.uk

ABSTRACT

The influence of iron on lead sulphide(PbS) and Copper Sulphide (CuS) thin films deposited on glass substrates via successive ionic layer adsorption (SILAR) Technique using lead acetate, $\text{Pb}(\text{CH}_3\text{COO})_2$, Cupric Acetate $\text{Cu}(\text{CH}_3\text{COO})_2$, thioacetamide ($\text{S}_2\text{H}_5\text{NS}$), Iron (II) Chloride dehydrate($\text{FeCl}_2 \cdot 2\text{H}_2\text{O}$), ethanol and ammonia by in alkaline medium annealed between 283K and 500K was investigated. The structural and morphological studies were performed by X-ray diffraction (XRD) Analysis and scanning electron microscopy(SEM) respectively. The Uv-visible studies were done using spectrometer in the Technical University, Ibadan. The XRD showed films of cubic crystalline PbS thin films, cubic and face-centred crystalline PbSFe thin films, cubic CuS thin film, hexagonal Cu_2S thin films and cubic and hexagonal crystalline natured CuSFe thin films with the preferential (111),(002)(004) (311) orientations.

INTRODUCTION

It is the energy crisis in the world that gave rise to the thin film growth research as a way to cushion problems associated with it. The continuous increase in population and industrialisation in almost every country in the world, has been very responsible for the ever growing

or increasing energy demand. In Nigeria, less than 40% of the country is connected to the national electric grid and less than 60% of the energy demand by this group is generated and distributed (Bala *et al.* 2008). The advantage of energy is facilitation of the provision of those things which are necessary for the welfare of human existence: health, heat, food, light, clothing, shelter and transport, etc. Energy availability improves the standard of living (Whitefield, 2000). Solar energy, an energy obtained from the sun, is the world's most abundant and cheapest source of energy available from Nature (Nwoke *et al.* 2008). It is free and automatically renewable every day. In the world over, emphasis has shifted from the use of hydro and fossil-powered electricity generation to renewable energy such as solar source through nanotechnology involving growing of thin films from the abundant transition metals, resulting in getting ones with excellent properties that will be useful in solving the problem of energy crisis (Jesuleye and Siyanbola, 2008). In the present study, lead sulphide and copper sulphide are studied to ascertain the structural and morphological properties when doped with iron. These new assumed properties will help determine their best areas of applicability. Lead sulphide (PbS) and Copper Sulphide (Cu_2S) are groups IV-VI and I-VI compounds of semiconducting materials respectively

(Liang and Whangbo, 1993) that have drawn attention of many researchers because of its properties that have been applied widely in optoelectronic devices, photoconductors, sensors, infra-red detector devices solar cells, solar control and solar absorber coatings (Chatterki *et al.* (2012), Koao *et al.* (2014), Preetha *et al.* (2015)). The present study describes successive ionic layer adsorption and reaction method for the synthesis and deposition of PbS, $(\text{PbS})_x(\text{Fe})_{1-x}$, CuS and $(\text{CuS})_x(\text{Fe})_{1-x}$

ternary thin films and the influence of iron added to the halide thin films structurally and morphologically. Variety of materials such as insulators, semiconductors, metals and temperature sensitive materials like polyester can be used as a substrate since the deposition is carried out at or near to room temperature. As it is a low temperature process, it avoids oxidation and corrosion of the substrate. In spite of this SILAR having a number of advantages as compared to other methods; it does not require vacuum at any stage, doping of any element can be achieved easily, film thickness can be easily controlled by adjusting the number of deposition cycles, operating at room temperature, no restrictions on substrate material, dimensions or its surface profile etc. The prime requisite for obtaining good quality thin film is the optimization of various preparative parameters viz. concentration of precursors, nature of complexing agent, pH of the precursor solutions and adsorption, reaction and rinsing time durations etc.(Valenzuela, 2003)

EXPERIMENTAL PROCEDURE.

The layer-by-layer growth of the material is achieved by dipping the substrate alternately into separately placed cationic and anionic precursors. After every cationic and anionic immersion the substrate is rinsed in deionised water to remove the un-adsorbed ions from the surface. The synthesis and deposition of PbS and CuS involved four steps while that of PbSFe and CuSFe thin films involved six steps. After pre-treatment of the substrates, the synthesis were done using .05M lead acetate and thioacetamide solution. Ammonia was used to control the pH. It was done between pH between 8.5 and 11.5. The iron ions were got from iron(II) chloride dehydrate. The copper ions were got

from cupric acetate. It was equally deposited in alkaline environment too.

For a SILAR growth of PbS thin film, only four steps are involved, namely:

- The glass substrate was first immersed in lead acetate solution for 35minutes , where lead ions were adsorbed on the surface of the substrate.
- The second step involves the rinsing of the substrate for 35 seconds in deionised water to remove loose and unadsorbed lead ions from the surface.
- The substrate was then immersed in thioacetamide solution for 35seconds, where the sulphur ions react with the pre-adsorbed lead ions on the substrate surface to form lead sulphide layer,
- Finally, the substrate was rinsed again with deionised water to remove unadsorbed and loose material from the substrate surface.
- A SILAR growth cycle for $PbS_x Fe_{(1-x)}$ thin films has six.steps, namely:
- The glass substrate was first immersed in lead acetate solution for 35 seconds , where lead ions were adsorbed on the surface of the substrate.
- The second step involves the rinsing of the substrate for 35 seconds in deionised water to remove loose and unadsorbed lead ions from the surface.
- The substrate was then immersed in thioacetamide solution for 35seconds, where the sulphur ions react with the pre-adsorbed lead ions on the substrate surface to form lead sulphide layer,

- Finally, the substrate was rinsed again with deionised water to remove unadsorbed and loose material from the substrate surface,
- The substrate was immersed in iron(II) Chloride dehydrate solution to adsorb iron ions on the pre-adsorbed lead sulphide layer,
- The unadsorbed iron ions were removed from the substrate by rinsing in deionised water for 35seconds.

After repeating for sufficient number of cycles(90 cycles), $PbS_x Fe_{(1-x)}$ composite thin films were deposited. The number of deposition cycles for PbS and Fe were adjusted to obtain various compositions of $PbS_x Fe_{(1-x)}$ thin films(see table 1 below)

Table 1. Deposition scheme for the growth of $PbS_x Fe_{(1-x)}$ thin films

Preparative Parameter	Cationic precursors		Anionic precursor
	$Pb(CH_3COO)_2$	$FeCl_{2.2H_2O}$	$S_2 H_5 NS$
Concentration(M)	0.05	0.05	0.05
pH	11.5	8.5	11.5
Immersion time (seconds)	35	35	35
Rinsing time (seconds)	35	35	35

Table 2. $PbS_x Fe_{(1-x)}$ thin films composition

Films	Composition parameter(x)	Number of SILAR cycles		Thickness (nm)
		PbS	Fe	
PbS	1.00	90	00	397
$PbS_{0.80}Fe_{0.20}$	0.80	80	10	393
$PbS_{0.50}Fe_{0.50}$	0.50	70	20	283
$PbS_{0.2}Fe_{0.8}$	0.20	60	30	299
$PbS_{.10}Fe_{.9}$	0.10	45	45	230

The thickness of the composite $(\text{PbS})_x(\text{Fe})_{(1-x)}$ thin film was measured by weight difference method. The density of PbS was taken as 4.9g/cm^3 and iron as 5.2g/cm^3 .

The densities of the composite $(\text{PbS})_x(\text{Fe})_{(1-x)}$ thin films were estimated by considering compositional parameter 'x'. The weights of the deposited films were determined by using an electronic microbalance. In the present investigation thickness of $(\text{PbS})_x(\text{Fe})_{(1-x)}$ films measured using sensitive microbalance is listed in table 2 above. The site for the research work was the crystal growth laboratory, Physics and Astronomy Department, University of Nigeria, Nsukka, Nigeria. The structural properties of the $(\text{PbS})_x(\text{Fe})_{(1-x)}$ composite thin films were studied by X-ray diffractometer with $\text{CuK}\alpha$ radiation of wavelength 0.154 nm . The surface morphological investigations were performed using scanning electron microscopy analysis and energy dispersive spectrometry (EDS) analysis at the Department of Industrial Chemistry, The Technical University, Ibadan Nigeria.

B. Copper Sulphide and Copper Sulphide Iron thin films.

The substrates were pre-treated as in the case above. For the SILAR deposition of $(\text{CuS})_{(1-x)}$ thin films, 0.05 M cupric acetate solutions were taken as cationic precursor and 0.05 M thioacetamide as anionic precursor. The pH of the anionic and cationic precursors was adjusted to 12 and 8 by ammonia addition. Substrate was immersed in the cupric acetate solution for 35 s to adsorb Cu^{2+} ions. (a) The un-adsorbed Cu^{2+} ions were removed from the substrate by rinsing it in deionised water for 35 s. (b) The substrate was then again immersed in thioacetamide solution for 35 s, where S^{2-} ions reacted with Cu^{2+} to form a layer of CuS. After repeating a sufficient number of cycles. It

was removed and dried in an oven to avoid dust and oxidation. For the SILAR deposition of $(\text{CuS})_{(1-x)}\text{Fe}_{(1-x)}$ thin films, the pre-treated glass substrates were immersed into 0.05 M cupric acetate solutions taken as cationic precursor, then rinsed in deionised water for 35 seconds before immersing into 0.05 M thioacetamide, taken as anionic precursor for 35 seconds before rinsing in deionised water. This was repeated for several cycles before the substrate was immersed in iron(II) Chloride dehydrate solution to adsorb iron ions on the pre-adsorbed copper sulphide layer.

The unadsorbed iron ions were removed from the substrate by rinsing in deionised water for 35seconds. It is worthy to note that the substrate was again immersed in thioacetamide solution where S^{2-} ions react with Cu^{2+} to form a layer of CuS. After repeating a sufficient number of cycles, $(\text{Fe})_{1-x}(\text{CuS})_x$ composite thin films were deposited. The number of deposition cycles for CuS and Fe was adjusted to obtain various compositions of $(\text{Fe})_{1-x}(\text{CuS})_x$.

Table 3: Deposition scheme for the growth of $\text{CuS}_x\text{Fe}_{(1-x)}$ thin films

Preparative Parameter	Cationic precursors		Anionic precursor
	$\text{Cu}(\text{CH}_3\text{COO})_2$	$\text{FeCl}_2 \cdot 2\text{H}_2\text{O}$	$\text{S}_2\text{H}_5\text{NS}$
Concentration(M)	0.05	0.05	0.05
pH	12	9	12
Immersion time (seconds)	35	35	35
Rinsing time (seconds)	35	35	35

Results and Discussion

Structural Characterisation.

The structural characterizations of $(\text{PbS})_x(\text{Fe})_{(1-x)}$ and $(\text{CuS})_x(\text{Fe})_{(1-x)}$ thin films were carried out using X-ray diffraction (XRD) technique. The peaks of XRD patterns have been assigned from the x-ray diffraction files ref. numbers : INEL/EZEMA/18-162115 and INEL/EZEMA/18-171343 respectively. Using the PbSFe as case study, detailed analyses are given in Tables 1 and 2 below. The crystallite size of the deposited material was calculated by using Debye- Scherer's formula (equation 2)

$$D = K\lambda / B\cos \theta, \quad (2)$$

where D is the average crystallite size, k is the particle shape factor that varies with the method of taking the breadth and shape of crystallites , λ is the X-ray wavelength used(0.1542 nm), β is the angular line width of half-maximum intensity (FWHM) of the diffraction peak, and θ is the Bragg's angle in degrees. See tables 1 and 2 below.

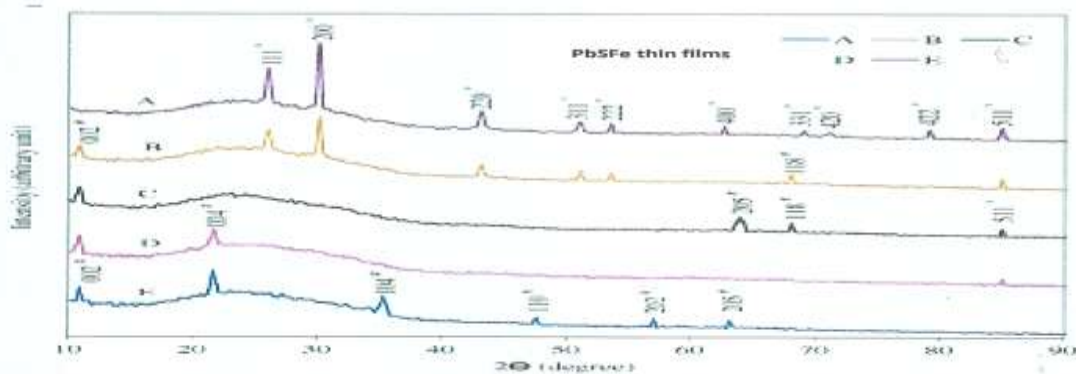


Figure 1. XRD of $(\text{PbS})_x(\text{Fe})_{(1-x)}$ composite thin films: (A) PbS, (B) $(\text{PbS})_{0.80}(\text{Fe})_{0.20}$, (C) $(\text{PbS})_{0.5}(\text{Fe})_{0.5}$, (D) $(\text{PbS})_{0.20}(\text{Fe})_{0.80}$ and (E) $(\text{PbS})_{0.10}(\text{Fe})_{0.90}$.

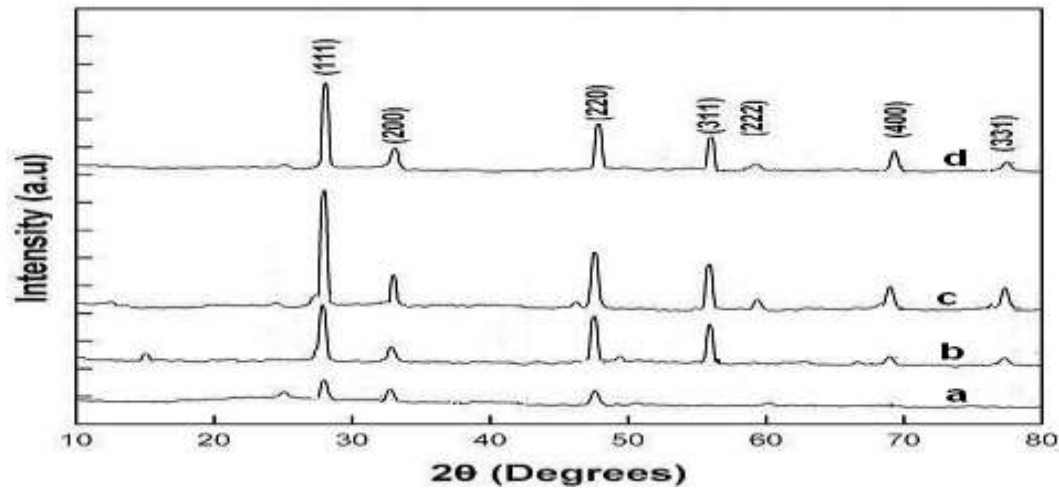


Figure 2 :XRD of $(\text{CuS})_x(\text{Fe})_{(1-x)}$ composite thin films: (a) $(\text{CuS})_{0.50}(\text{Fe})_{0.50}$ (b) $(\text{CuS})_{0.20}(\text{Fe})_{0.80}$, (c) $(\text{CuS})_{0.1}(\text{Fe})_{0.9}$, (D) CuS

Table 1. Thickness, grain size, strain and dislocation density of $(\text{PbS})_x(\text{Fe})_{(1-x)}$ thin films.

Film composition	Thickness (nm)	Grain Size (nm)	Dislocation density ($\delta \times 10^{10}$ lines/cm ²)	Strain ($\epsilon \times 10^{-4}$)
A PbS	375	34	10.91	10.17
B $(\text{PbS})_{0.80}(\text{Fe})_{0.20}$	301	26	14.26	14.30
C $(\text{PbS})_{0.5}(\text{Fe})_{0.5}$	290	25	15.99	14.77
D $(\text{PbS})_{0.20}(\text{Fe})_{0.80}$	285	18	16.87	14.90
E $(\text{PbS})_{0.10}(\text{Fe})_{0.90}$	280	16	32.47	21.03

Table 2. Thickness, grain size, strain and dislocation density of $(\text{CuS})_x (\text{Fe})_{(1-x)}$ thin films.

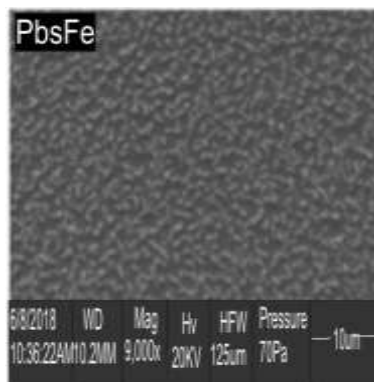
Film composition	Thickness (nm)	Grain Size (nm)	Dislocation density ($\delta \times 10^{10}$ lines/cm ²)	Strain ($\epsilon \times 10^{-4}$)
A CuS	386	35	10.47	10.17
B $(\text{CuS})_{0.80}(\text{Fe})_{0.20}$	300	33	14.66	11.30
C $(\text{CuS})_{0.5}(\text{Fe})_{0.5}$	298	30	15.92	13.77
D $(\text{CuS})_{0.20}(\text{Fe})_{0.80}$	287	19	17.57	14.99
E $(\text{CuS})_{0.10}(\text{Fe})_{0.90}$	273	17	32.47	21.34

Morphological Studies

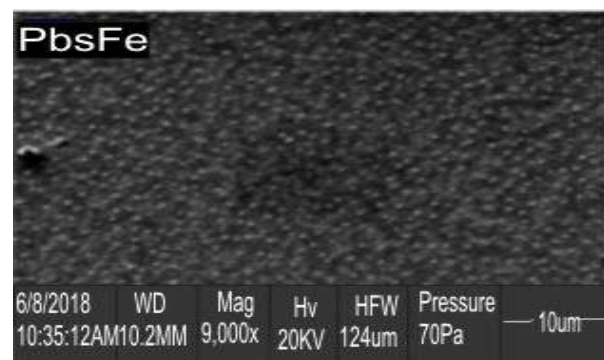
The morphological characterisation of CuS, CuSFe, PbS and PbSFe thin films were done using the scanning electron microscopy analysis(SEM) and Energy Dispersive spectrometry analysis .

Scanning electron microscopy(SEM) analysis

The SEM Micrographs of the doped and undoped PbS and CuS thin films are show in Figures 3 and 4 below:



(A)



(B)

Figure 3. SEM images of $(PbS)_x(Fe)_{(1-x)}$ composite thin films: (A) $PbS_{0.20}(Fe)_{0.80}$ at $10\ \mu m$ (HFW=125 μm) (G) $(PbS)_{0.8}(Fe)_{0.2}$ at $10\ \mu m$ (HFW=124 μm)

SEM of doped CuS thin film SILAR (deposited at 90cycles) is shown below in Figure 6 below.



Figure 4. SEM Micrograph of CuSFe (A) micrograph at 15 μm (B) micrograph at 20 μm

3.2.2 Energy Dispersive Spectrometry (EDS) Analysis : These are show in Figures 7 and 8 below.

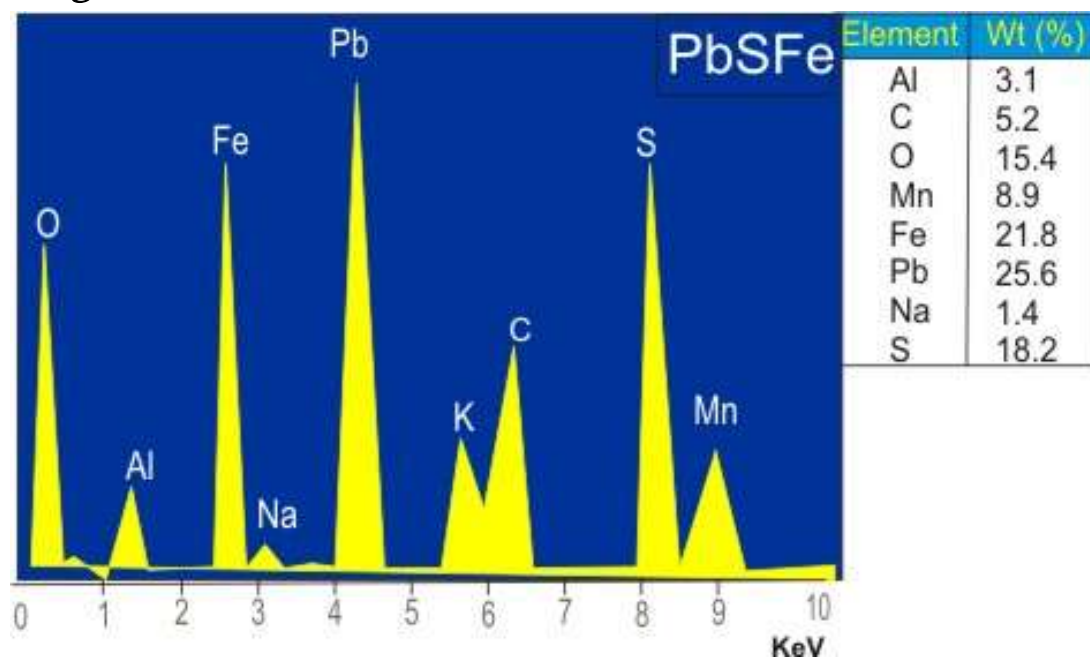


Figure 5. EDS of $(PbS)_x(Fe)_{(1-x)}$ composite thin films:

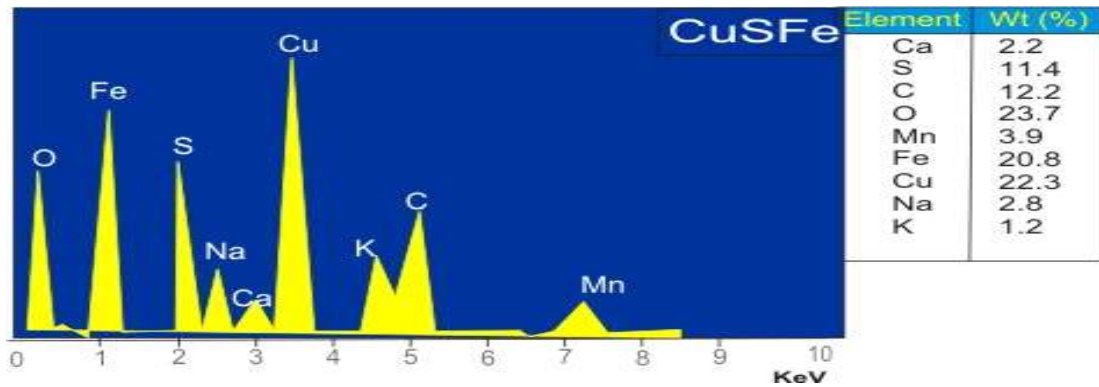


Figure 6. EDS of $(\text{CuS})_x(\text{Fe})_{(1-x)}$ composite thin films.

3.3 Optical characteristics

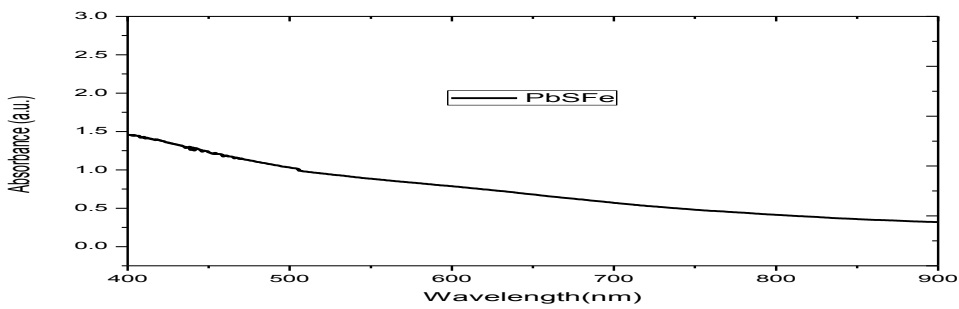


Fig 7: Plots of absorbance against wavelength for PbSFe thin film

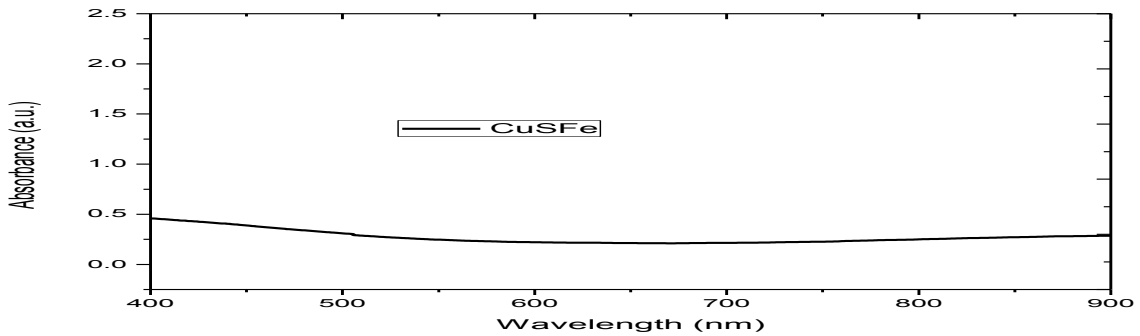


Fig 8: Plots of absorbance against wavelength for CuSFe thin film

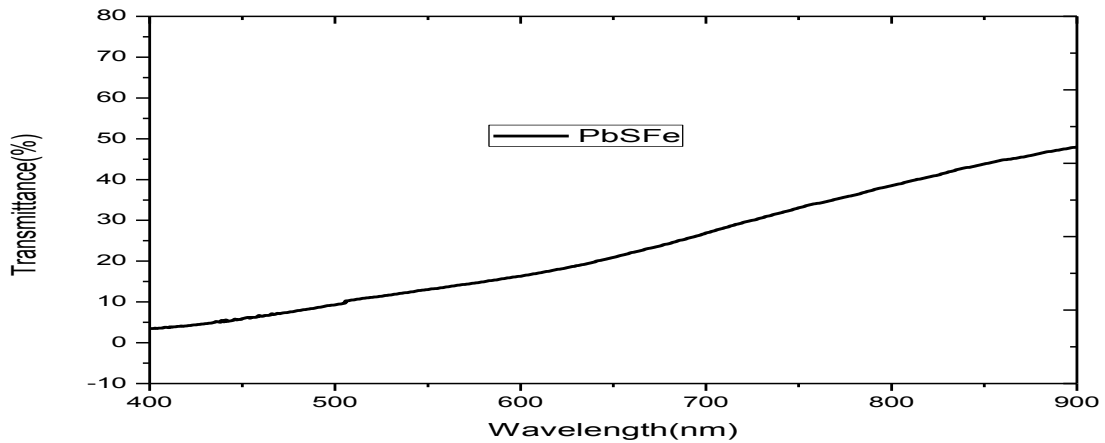


Fig 9: Plot of transmittance against wavelength for PbSFe thin films

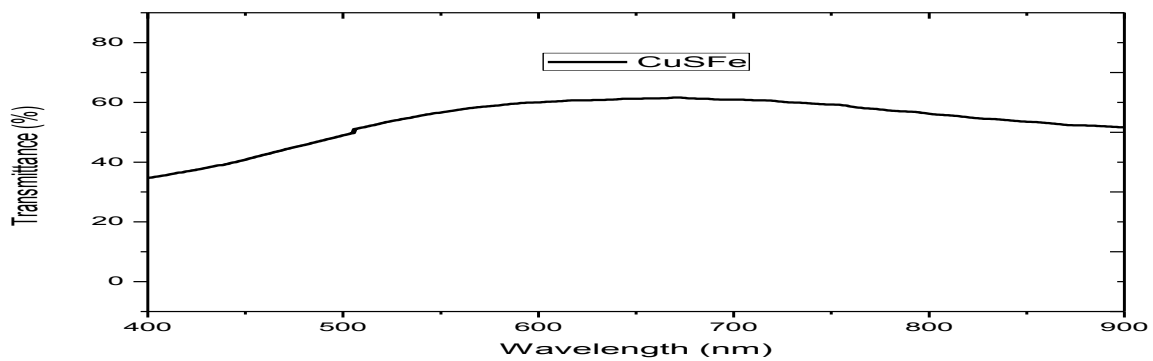


Fig 10 : Plot of transmittance against wavelength for CuSFe thin films

Fig.7 shows the plots of absorbance against wavelength of PbSFe thin films while Figure 9 depicts the plots of transmittance against wavelength. Figure 8 shows the plot of absorbance against wavelength of CuSFe thin films while Figure 10 depicts the plots of transmittance against wavelength for CuSFe thin films. The absorbance spectra of PbSFe thin films (Fig.7) vary in a manner, decreasing continuously from 1.40 (a.u) at 400nm to about 0.50 at 900nm. This range of absorbance is in agreement with the reports of Uhugebu (2007) for FePbS thin films, Agbo and Nnabuchi (2011) for TiO_2/PbO thin films,

and Onah,Ugwu and Ekpe (2015) for TiO_2/CuO thin films. The absorbance spectra of CuSFe thin films (Fig.8) shows that the thin films decreased with wavelength within 400–500nm and then remained fairly constant within the wavelength range 550–700nm. Thereafter, it increased within the wavelength range 750–900nm. The maximum absorbance is about 0.5 (a.u.) at 400nm. This value of absorbance is below the maximum of 1.50 (a.u) by Uhuegbu (2007) for FeCuS_2 thin films. The high absorbance displayed by PbSFe films may be used as spectrally selective coating for solar thermal applications. Solar collectors for heating fluids require increasing the reception area of the solar radiation, and/or to increase the absorbance of the surface coating in order to improve thermal efficiency (Oliva, Maldonado, Diaz and Montolvo, 2013).

The graph of transmittance against wavelength was plotted as shown in Fig.9 for PbSFe thin films and Fig. 10 for CuSFe thin films. The transmittance of PbSFe thin films increased with wavelength reaching a peak of about 9% in the infrared region. This value of transmittance is far lower compared to the report of Uhuegbu (2007) for FePbS thin films. However, it is within the range with that of Augustine and Nnabuchi (2017) for PbS/NiO/CdO thin films. The low transmittance of PbSFe thin film is expected since the absorbance is high and both optical parameters have inverse relationship. The transmittance spectra of PbSFe thin films vary in a manner involving significant improvement in percentage transmittance from 4% to about 47% was observed. These findings are in agreement with that of Augustine and Nnabuchi (2018) for CuO/PbS thin films and Nnabuchi and Augustine (2018) for $\text{Mn}_3\text{O}_4/\text{PbS}$ thin films. The transmittance spectra for CuSFe thin films (Fig. 10) vary in different manner, increasing from about

35% at 400 nm to about 58% in the wavelength range 550nm and then remained fairly constant in the wavelength range 575–750nm. Thereafter, it decreases to about 52% at 900nm. Generally, PbSFe and CuSFe thin films transmit well. The relatively high transmittance of PbSFe and CuSFe thin films in the infrared region suggest that they may be used for coating the walls and roofs of poultry houses to facilitate the transmission of infrared radiation in order to generate the heat required for warming young chicken. This has the potential to reduce the cost of energy consumption associated with the use of electric bulbs, stoves and lamps. These findings are in agreement with the report of Augustine and Nnabuchi (2018) for CuO/PbS thin films.

SUMMARY:X-ray diffraction patterns ofCuSFe and $(\text{PbS})_x(\text{Fe})_{1-x}$ composite films were shown in Fig.1 and 2 above. The peaks of XRD patterns have been assigned from the x-ray diffraction files ref. numbers : INEL/EZEMA/18-162115 and INEL/EZEMA/18-171343 respectively. Lead sulphide thin film has ten diffraction peaks (111)(200) (220) (311) (222)(400) (331)(420)(422)(511), which corresponds to 2θ angles ranging from10.098–85.846. The XRD of doped PbS and CuS annealed at about 650K has been included. These had thirteen and seven peaks ranging from angles 2θ ranging from 10.429–85.9645 and 18.012–80.012 respectively. The (0 0 2) and (0 0 4) orientations due to hexagonal lattice are prominent in CuSFe and (1 1 1) and (2 0 0) orientations due to cubic lattice are distinct in pure PbS and CuS thin films. The PbSFe thin films annealed at temperature less than 500K were crystals that was cubic and face-centred. However, at $x = 0.5$ i.e. for $(\text{PbS})_{0.5}(\text{Fe})_{0.5}$, and $(\text{CuS})_{0.5}(\text{Fe})_{0.5}$ strong orientations disappear showing the non-formation of crystals

due to the sp-d orientation. The crystallite sizes of the deposited materials were calculated using Debye-Scherer's formula.

Thickness for PbS , (PbS)_{0.8}(Fe)_{0.2} , (PbS)_{0.5}(Fe)_{0.5}, (PbS)_{0.2}(Fe)_{0.8}, (PbS)_{0.1}(Fe)_{0.9} were 375nm,301nm, 290nm, 285nm and 280nm while their grain sizes were 34, 26, 25, 18,16 . Their dislocation density(ρ) calculated were 10.91,14.26, 15.99, 16.87 and 32.47 respectively. The strain were calculated as 10.77, 14.30,14.77,14.90 and 21.03 respectively while thickness for CuS, (CuS)_{0.8}(Fe)_{0.2} , (CuS)_{0.5}(Fe)_{0.5}, (CuS)_{0.2}(Fe)_{0.8}, (CuS)_{0.1}(Fe)_{0.9} . were 386, 300, 298,287,273 while their grain sizes were 35, 33, 30, 27, 19,17. The variation in the strain and dislocation density may influence the properties on the nanostructures. The compositional analysis showed that the iron content of the SILAR synthesized PbSFe thin films was 21wt % and CuSFe thin films was 20.8wt%.

From literature, the lead Sulphide thin films have been reported as having thermal stability as observed in this study. The samples(doped and undoped) were annealed between temperatures of 293K and 493K and from the XRD, the intensity ratio some diffractions changed but no additional peaks were observed up to 475K; This showed that the PbS nanofilm was not oxidized. The change in the diffraction reflection intensities was attributed to the fact that the phase transition to cubic structure takes place in the PbS film at 375K (Qadri et al. 2003).

The presence of oxygen atoms as shown by the EDS studies showed that the proportion of iron to lead sulphide and iron to copper sulphide were not in equal proportion and also oxidation must have taken place because of their large surface area(Qadri et al. 2003). Based on this finding, the lead sulphide thin films (doped and undoped) can be used

in devices as fire alarm sensors, flame sensors and heat source detection systems.

CONCLUSIONS

A simple, cheap and convenient SILAR method was employed to deposit good quality CuSFe and $(\text{PbS})_x(\text{Fe})_{1-x}$ composite thin films. The deposited films were uniform and adherent to the substrate. Their structural and morphological properties of those composite thin films were studied. The EDS Studies showed that in $(\text{PbS})_x(\text{Fe})_{1-x}$ composite thin films, the composition of iron was 21.8wt% while in $(\text{CuS})_x(\text{Fe})_{1-x}$ composite thin films, iron composition was 20.8wt%. The XRD and morphological studies revealed that CuSFe and $\text{PbS}_x(\text{Fe})_{(1-x)}$ thin films were nanocrystalline in nature depending on film composition. The average crystallite size was found to vary for the CuSFe thin films between 35 and 17 nm and for PbSFe thin films 34 and 16 depending on film composition. The variation in thickness, strain and dislocation densities were also composition dependent. Similar observation has been reported by Wang et al. The samples annealed at different temperatures (383K–500K) never showed any prominent peaks structurally and morphologically as confirmed by studies done by He *et al.*, From literature, considerable changes can be seen for temperatures up to 700 °K (Mote, 2012). The high absorbance displayed by PbSFe films may be used as spectrally selective coating for solar thermal applications. Solar collectors for heating fluids require increasing the reception area of the solar radiation, and/or to increase the absorbance of the surface coating in order to improve thermal efficiency. The relatively high transmittance of PbSFe and CuSFe thin films in the infrared region suggest that they may be used for coating the walls and roofs of poultry houses to facilitate the transmission of

infrared radiation in order to generate the heat required for warming young chicken. These properties can be well used in solar energy conversion devices and optoelectronics.

ACKNOWLEDGMENT

The authors are grateful to Nanoscience Research Group, University of Nigeria Nsukka

REFERENCES

- Adegbenro, O. (2011). Challenges and Prospect of Energy Efficiency and Conservation. *Journal of Energy Policy, Research and Development*, 1(1), 104-110.
- Akujor, C (1988): Energy Technology, *Summer Educational Publishers (Nig.) Limited*, Onitsha..1,4-6
- Bala, E.J., Ojosu, J.O., and Umar, I.H., Government Policies and Programmes on the Development of Solar PV Sub-sector in Nigeria.(2008) *Nigeria Journal of Renewable Energy*, 8(1 and 2): 1-6.
- Boer, K.W.,(1977), *Physica Status Solidi*. A40, 435.
- Chaudhuri, T. K. and Chatterjes, S. (1992).Ternary Thin Films, *Proceedings of the International Conference on Thermoelectronics*. New Jersey,N.Y, 11: 40.
- Fernandes, P.A., Salome, P.M. and Cunha, A.F. (2010). A study of ternary Cu_2SnS_3 and Cu_2SnS_4 thin Films prepared by sulphurizing stacked metal precursors, *Journal of Physics D: Applied Physics*, 43, 1-11.
- He, Y, Yu, X and Zhao, X. (2007), *Materials latter*, 61, 3014

Ibrahim, S. G. and Salame, P. H. (2016). Thickness Dependent Physical Properties of lead Sulphide thin Films, *Int. J. Chemistry*, 6:5-11

Jesuleye, A.O. and Siyanbola, W.O. (2008). Solar Electricity Demand Analysis for Improved Access to Electricity in Nigeria.. *Nigeria Journal of Solar Energy*. (1): 136-141.

JCPDF Powder Diffraction File search manual – 2003, 89-2073.

Mote, V., Y. Purushotham, Y., and Dole, B.(2012), The morphological, optical and electrical properties of nanocrystalline PbS thin films., *J. Theor. Appl. Phys.* 6, 1 7.

Nicolau, Y. F, Dupuy M, Brunel, M (1990): *Journal of Electrochemical society*, 137, 2915.

Oji J. O, Nascu, C., Pop, I.and Ionescu, V. (2012). Utilisation of Solar Energy for Power Generation in Nigeria. *International Journal of Energy Engineering*, 2(2):54-5

Liang,W and Whangbo, M.H(1993): *Solid State Communications*. 85 (1993) 405

Nwoke, O. O., Okonkwo, W. I. and Oparaku, O. U. (2008). Solar Energy Use in Nigeria: constraints and Possible Solutions. *Nigeria Journal of Solar Energy*, 19(1), 90-93.

Nair, M T.S, Alvarez-Garcia,G., Estrada-Gasva C.A. and Nair, P.K(1993); *Journal of Electrochemical Society*. 140, 212.

Nair, P.K., Garcia, V.M., Fernandez, A. M. Ruiz H.S and Nair, M.T.S (1991), *Journal of Physics D*. 24, 441.

- Han, Z.H. Li, Y.P., Zhao, H.Q., Yu, S.H., Yin, Y.L., and Qian, Y.T(2000),
Materials Letters. 44, 366.
- Okafor, E.C.N. and Joel-Uzuegbu, C.K.A.(2010). Challenges to
Development of Renewable Energy for Electric Power Sector in
Nigeria. *International Journal of Academic Research*. 2(2): 211-
216.
- Qadri, S. B. , Singh, A. and Yousuf, M.(2003): Structural stability of PbS
Films as a function of temperature, *Thin Solid films*,
431(432),506-510
- Wang, S.Y, Wang, W,Lu,Z.H(2003):*Material Science and Engineering*,
B10,3184
- Okonkwo, W. I. Passive Passive Solar Heating, for Poultry Chick
Brooding in Nigeria. A Paper presented at the *International
Workshop on Renewable Energy for Sustainable Development in
Africa*, 2nd May, 2007
- Olivia, A. I., Maldonado, R. D., Diaz, E. A. and Montolvo, A. I. (2013). A
high absorbance material for solar collector's applications,
Materials Science and Engineering, 45, 1-4.
- Onah, D. U., Ugwu, E.I. and Ekpe, J. E. (2015). Optical Properties of
Nanocrystalline TiO₂/CuO Core-Shell Thin Films by Thermal
Annealing, *American Journal of Nano Research and Applications*,
3(3), 62-65.
- Sambo, A.S (2008). The Role of Energy in achieving Millenium
Development Goals (MDG): Keynote Address of the *National
Engineering Conference (NETEC)*, Ahmadu Bello University, Zaria,
1st April, 2008.

- Smith, G. B., Ignatiev, A. and Zajac, G.(1980).Copper sulphide nanocrystalline thin films at room temperature, *Thin Solid films*, 514, 132-137.
- Whitefield, D. (2000). Solar Dryer System and the Internet Important Resources to Improve food preparation. A Paper presented at *International Conference on Solar Cooking, Kimberly, South Africa*, and 24th June, 2000.
- Valenzuela, J., J'auregui, R., Ram'irez-Bon, A., Mendoza-Galva'n, M. and Sotelo-Lerma, A. (2003). Optical properties of PbS thin films chemically deposited at different temperatures. *Thin Solid Films*, 1441: 104-110.
- Yucel, E., Yucel, Y., Beleli, B.(2015). Process optimization of deposition conditions of PbS *Appl. Phys. Lett.*, 56, 51-53.

Reference to this paper should be made as follows: Udeajah, V.N. and Onah, D.U (2018), Structural, Optical Absorbance and Transmittance Properties of Silar Deposited Iron Lead Sulphide(PbSFe) and Ironcopper Sulphide(CuSFe) Thin Films. J. of Physical Science and Innovation, Vol. 10, No. 3, Pp. 13-33
